

DAA/ LANGLEY

FU 200635

IN-26

69618-CR

P.24

Investigation of Temperature and  
Concentration Oscillations in the Directional  
Solidification of Pb-Sn-Te

Semi-Annual Progress Report

August 1, 1986 - January 31, 1987

Grant: NAG-1-609

T.J. Anderson, Principal Investigator  
R. Narayanan, Co-Principal Investigator  
Department of Chemical Engineering  
University of Florida  
Gainesville, FL 32611

(NASA-CR-180565) INVESTIGATION OF  
TEMPERATURE AND CONCENTRATION OSCILLATIONS  
IN THE DIRECTIONAL SOLIDIFICATION OF  
Pb-Sn-Te Semiannual Progress Report, 1 Aug.  
1986 - 31 Jan. 1987 (Florida Univ.) 24 p

N87-26209

Unclas  
0069618

G3/26

INVESTIGATION OF TEMPERATURE AND CONCENTRATION  
OSCILLATIONS IN THE DIRECTIONAL SOLIDIFICATION  
OF Pb-Sn-Te

ABSTRACT

Directional solidification of the pseudobinary compound semiconductor material  $\text{Pb}_{1-x}\text{Sn}_x\text{Te}$  by the Bridgman crystal growth process will be studied. Natural convection in the molten sample will be visualized with a novel electrochemical cell technique that employs the solid electrolyte material yttria-stabilized zirconia. Mass transfer by both diffusion and convection will be measured by detecting the motion of oxygen tracer in the liquid. Additional applications for electrochemical cells in semiconductor crystal growth are suggested. Unsteady convection in the melt will also be detected by the appearance of temperature oscillations. The purpose of this study is to experimentally characterize the overstable conditions for a  $\text{Pb}_{1-x}\text{Sn}_x\text{Te}$  melt in the vertical Bridgman crystal growth technique and use a linear analysis to predict the onset of convection for this system.

## Project Description

### 1. INTRODUCTION

Elemental semiconductor materials, especially silicon, are well understood and allow relatively easy processing, and will therefore continue to be dominant in electronic systems in the foreseeable future. They suffer from certain inherent limitations, however; chiefly because their elemental nature does not allow much freedom of choice in constructing semiconductor devices. An obvious step toward greater freedom is the use of compound semiconductor materials, where the desired properties can be attained by fixing the composition of the material. One such compound semiconductor is lead tin telluride ( $\text{Pb}_{1-x}\text{Sn}_x\text{Te}$ ), a direct bandgap material that is used as an infrared detector and emitter (laser or LED). The desirable features of  $\text{Pb}_{1-x}\text{Sn}_x\text{Te}$  are its narrow bandgap, which gives a long wavelength (2.5 to 28 micrometers), and its wavelength tunability, which is achieved either internally by varying the composition (the value of  $x$ ) or externally by varying the temperature, pressure, or applied magnetic field.<sup>(1)</sup> Both features are important in high resolution spectroscopy (specifically, atmospheric monitoring), which is one application of this compound semiconductor material.

$\text{Pb}_{1-x}\text{Sn}_x\text{Te}$  crystals are commonly grown by a variation of the Bridgman technique in which a molten sample in a cylindrical ampoule is directionally solidified by moving the ampoule in its axial direction through a temperature gradient. Typically, the direction of motion is vertical which allows the choice of whether the hotter end of the temperature gradient will be at the top or at the bottom of the sample. The temperature gradient is produced with a three-zone furnace: a hot (above the melting point) zone and a cold (below

the melting point) zone separated by an insulated zone that makes the temperature gradient more linear.

It is convenient to consider  $\text{Pb}_{1-x}\text{Sn}_x\text{Te}$  as a pseudobinary solution of the compounds PbTe and SnTe. The phase diagram<sup>(2)</sup> shows that at all temperatures and compositions the liquid has a higher concentration of SnTe than the solid. During solidification the liquid will gradually become richer in SnTe as the PbTe freezes preferentially into the solid. The concentration profile in the solid after directional solidification will be somewhere between two limiting cases. The first case is the most common; it is when composition redistribution in the liquid melt, due chiefly to convection, occurs faster than solidification, and any concentration change at the liquid-solid interface quickly affects the entire liquid. The liquid is considered to be fully mixed at all times, and the resulting solid composition is expressed by the normal freezing equation

$$C = kC_0(1 - g)^{k-1} \quad (1)$$

where  $C$  is the concentration in the solid of one component of the solution,  $C_0$  is the concentration in the sample before freezing begins,  $g$  is the fraction of the sample solidified and  $k$  is the segregation coefficient, that is, the ratio of the concentration in the solid to the concentration in the liquid at the interface.<sup>(3)</sup> In  $\text{Pb}_{1-x}\text{Sn}_x\text{Te}$  the segregation coefficient is nearly constant. The normal freezing case is shown graphically in Figure 1. The other, more unusual limiting case occurs when there is no convection in the liquid and composition redistribution is by diffusion only. This case has been examined by Tiller, et al.,<sup>(4)</sup> and is shown graphically in Figure 2. Most directionally solidified samples follow closely the first case but it

would be preferable if the second case could be achieved. Most of the resulting solid would then be of a constant composition and would therefore be more easily used for mass production of semiconductor devices.

To achieve the second case, where composition distribution is by diffusion only, convection in the liquid must be suppressed, and this requires an understanding of the forces that drive convection. The strongest driving force for convection is gravity acting on density gradients in the molten material. Density gradients in  $\text{Pb}_{1-x}\text{Sn}_x\text{Te}$  arise in two ways: thermally and solutally. Thermal density gradients occur because the density of the liquid decreases with increasing temperature, so the temperature gradient used in Bridgman crystal growth causes a density gradient. If the bottom of the sample is hotter than the top, gravity opposes the density gradient, the liquid is thermally unstable and convection occurs. Solutal density gradients occur because the density of the liquid decreases with increasing SnTe concentration. As the sample freezes, the liquid adjacent to the liquid-solid interface becomes richer in SnTe and therefore less dense. If the interface is at the bottom of the liquid, gravity opposes the density gradient, the liquid is solutally unstable and convection occurs. The directions of thermal and solutal instability oppose one another, so convection occurs whether the sample is hotter at the top or at the bottom.<sup>(5)</sup> It is hoped that both convective forces would be greatly diminished when crystal growth is performed in the microgravity environment of space. To this end, crystal growth experiments are being performed both on the ground and in space. Ground-based experiments have exhibited normal (convective) freezing, while space-based experiments have so far been inconclusive.

The preceding qualitative description can be replaced with a more quantitative understanding by application of theory and by careful experimental

measurement. The differential equations that are used to model fluid flow are well known and cases of liquid convection similar to Bridgman crystal growth have been discussed in the literature;<sup>(6)</sup> however, analytic solutions to the fluid flow equations have not been possible without excessively simplifying assumptions. Current research includes numerical approaches to mathematical modelling of convection in the liquid.<sup>(7,8)</sup> The accuracy of an analytic or numeric mathematical model is judged by comparison with experimental results. Much of the experimental work is limited to post-growth analysis of the resulting solid sample, which includes chemical etching to reveal the shape and position of the solid-liquid interface during growth, measurement of the solid composition by electron microprobe analysis, and X-ray diffraction studies to determine the orientation and quality of the crystals. Measurement of convection during growth has until now been limited to the use of thermocouples to follow changes and oscillations in the liquid temperatures.<sup>(5)</sup>

In compound semiconductors the quality of the final material is very dependent on composition variations in the molten sample during crystal growth. It is proposed that convection during Bridgman crystal growth be monitored with thermocouple and electrochemical concentration cells. It is hoped that data from these measurements could be used to follow convection flow patterns in the liquid. The formulation of the analytical problem is first presented. The experimental progress to date and proposed work is then summarized.

## 2. FORMULATION OF ANALYTICAL PROBLEM

The system that will be analyzed is shown in Figure 3. The following assumptions will be made in this study:

- 1) the gas phase is inviscid and the liquid phase is a binary Newtonian fluid,
- 2) viscous dissipation is negligible,
- 3) density is a linear function of temperature and concentration,
- 4) the surface tension is sufficiently high to assume a flat interface,
- 5) morphological stabilities will not be considered,
- 6) the temperature and velocity fields are axisymmetric,
- 7) heat flow is 1-dimensional in the axial direction, and
- 8) Marangoni convection can be neglected.

The last three assumptions are especially important. The analysis of Schlüter, Lortz, and Busse<sup>(9)</sup> predict that 2-dimensional rolls are the only stable configuration for buoyancy-driven convection in an infinite layer of fluid with temperature independent properties. Also, Hoard, Robertson, and Acrivos<sup>(10)</sup> observed a symmetric roll pattern for deep layers of fluid with highly temperature dependent viscosity. Thus, it appears likely that flow will develop in an axisymmetric manner.

One-dimensional heat flow is necessary for obtaining a possible conductive state without radial gradients at the interface. Several steps have been taken to ensure axial heat flow: a large thickness of Shuttle tile insulation is used between the thermal zones of the furnace (Fu and Wilcox<sup>(11)</sup>), insulation has been added to the sidewalls of the quartz to cut down on radial heat transfer, and efforts have been made to extend the constant gradient zone and decrease the radial heat flux from the hot zone to the end of the sample. Lastly, Marangoni effects on Earth are generally dominated by buoyancy effects, except for very thin layers, and can be neglected completely for the hot on top case.

The governing equations for this problem in non-dimensional form are:

### Continuity

$$\nabla \cdot \mathbf{V} = 0 \quad (2)$$

### Motion

$$\frac{1}{Pr} \frac{\partial \mathbf{V}}{\partial t} + \mathbf{V} \cdot \nabla \mathbf{V} = -\nabla P + \frac{Ra}{Pr} T \bar{\mathbf{F}} + \frac{Ra_s}{Sc} C \bar{\mathbf{F}} + \nabla^2 \mathbf{V} \quad (3)$$

### Energy

$$\frac{Pr}{Sc} \frac{\partial T}{\partial t} + Pr (\mathbf{V} \cdot \nabla T) = \nabla^2 T \quad (4)$$

### Species

$$\frac{\partial C}{\partial t} + Sc (\mathbf{V} \cdot \nabla C) = \nabla^2 C \quad (5)$$

$\mathbf{V}$ ,  $C$ , and  $T$  are the velocity, concentration, and temperature field.  $\bar{\mathbf{F}}$  is a unit force in the direction of gravity and  $t$  is time. These equations have been obtained by using the following characteristic variables:

$$\mathbf{V} = \mathbf{V}'L/\nu$$

$$P = P'L^2/(\rho C_p L^2)$$

$$C = (C' - C_2)/(C_1 - C_2)$$

$$T = (T' - T_2)/(T_1 - T_2)$$



$$t = t'D/L^2$$

where primed variables are dimensional and  $T_1$  and  $T_2$  are temperature at the top and bottom surfaces, respectively.

Care should be taken in choosing the characteristic variables. For instance, the  $Pr/Sc$  term that precedes the time derivative in eqn. (4) is approximately 0.004 ( $Pr=1$ ,  $Sc=25$ ). As a result, almost all of the time dependence of the temperature field is supplied by the interrelated motion (3) and species (5) equations. Thus, one could infer that the temperature field and concentration will be kept "in phase," with the fluctuations in temperature following closely those of concentration. If the time had been scaled with thermal diffusivity, though, the  $Pr/Sc$  term in eqn. (4) would not have appeared and the above relationship would have gone unnoticed. Instead, a  $Sc/Pr$  term would have preceded  $\partial C/\partial t$  with relatively little insight gained. The purpose of this study will be to use Green's functions in order to solve the problem in the form of an integral equation.

### 3. EXPERIMENTAL DETERMINATION OF TEMPERATURE OSCILLATIONS

The ampoule used in these experiments is a vertical circular cylinder of fused silica (quartz). Preliminary furnace experiments have been run with molten tin as the fluid phase in a destabilizing temperature gradient. A small amount of purified argon is trickled through the cell to prevent contamination of the tin with oxygen. Insulation is placed on the outside wall of the cell in order to reduce radial temperature gradients. Cotronics ceramic board is used to make insulating spacers that hold the Cotronics insulation blanket in place. The insulating board and blanket have thermal conductivi-

ties of  $3.28 \times 10^{-4}$  cal/°C-cm-sec and  $4.83 \times 10^{-4}$  cal/°C-cm-sec, respectively. The quartz, on the other hand, has a much higher thermal conductivity of  $7.75 \times 10^{-3}$  cal/°C-cm-sec. Furthermore, the cell is placed in the Shuttle tile ( $k = 3.90 \times 10^{-4}$  cal/°C-cm-sec) insulation zone of the furnace. Heat flow is made more 1-dimensional in this zone due to the long insulation zone (65 mm or 8R). Finally, isothermal heat pipes are used in the heating zones of the furnace to reduce temperature roll off at the Shuttle tile-heater block boundary. Reducing this roll off lengthens the constant gradient region which reduces the inward heat flux from the hot zone into the side of the cell (Rouzaud, Camel, and Favier).<sup>(12)</sup> The combination of these three effects should ensure axial heat flow through the cell.

Chromel-alumel (type K) thermocouples are placed between the quartz wall and the insulation blanket at one cm intervals in the vertical direction. The thermocouples are used to measure temperature, the temperature gradient in the melt, and to detect temperature fluctuations (hence, unsteady convection). The temperatures are recorded at 5-minute intervals and one of the channels is monitored by a Data 6000 recording waveform analyzer at 2-second intervals. An FFT can be run on the data

The thermal gradient is slowly increased until the temperature fluctuations appear on the Data 6000. When oscillations are detected, the Rayleigh number is calculated. The temperatures used in these calculations have not yet been corrected for the temperature drop that is caused by the quartz wall (probably on the order of 10°). Since the relevant physical properties of tin have a weak temperature dependence for  $T > 260^\circ\text{C}$  and the gradient measured in this way should be close to the value inside the tube, the value calculated for the Rayleigh number should be a reasonable approximation. Critical Rayleigh numbers ( $Ra^{c2}$ ) calculated for  $AR = 3.15$  and  $AR = 5.0$  are approximately 135,000 and 220,000 respectively.

Further experiments will involve taking temperature measurements from a  $\text{Pb}_{.8}\text{Sn}_{.2}\text{Te}$  crystal growth system to determine  $\text{Ra}^{c2}$  and  $\text{Ra}_s^{c2}$ . This data will be used to qualitatively verify results from the theoretical analysis. Other important experiments would include determining the density change of LTT upon freezing ( $\epsilon = 1 - \rho_s/\rho_L$ ) and determining the extent of the radial temperature gradient. The importance of radial gradients has been discussed previously. One method of measuring  $\partial T/\partial r$  will be to place a thermocouple in a capillary tube in the middle of the tin cell at the same axial position as a thermocouple placed on the side of the cell. This cell will be heated from above, since the onset of axisymmetric convection in the thermally unstable case would produce a misleading radial gradient.

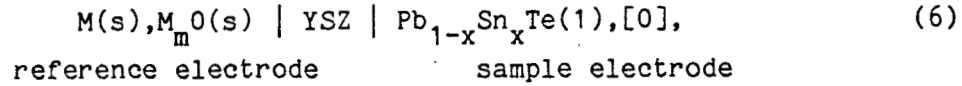
If  $\epsilon$  is sufficiently large (say greater than .05), it can be an important cause of convection. Thus, it is necessary to measure accurately to determine whether or not to include this effect in future models. One proposed method of measuring  $\epsilon$  involves using a laser to mark the solid-liquid interface in a see-through furnace and recording the movement with a VCR camera.

#### 4. EXPERIMENTAL DETERMINATION OF CONCENTRATION OSCILLATIONS

The electrochemical cells use a solid electrolyte technique that has been applied in a variety of thermodynamic studies.<sup>(13)</sup> The most popular solid electrolyte has been zirconia ( $\text{ZrO}_2$ ) stabilized by the addition of oxide dopants such as calcia ( $\text{CaO}$ ), magnesia ( $\text{MgO}$ ), or yttria ( $\text{Y}_2\text{O}_3$ ). These dopants create anion vacancies in the zirconia lattice and at sufficiently high temperatures ( $>600^\circ\text{C}$ ) oxygen anions ( $\text{O}^{2-}$ ) can move through the electrolyte by migrating from vacancy to vacancy, while zirconia's low porosity prevents the transfer of other species.<sup>(14)</sup> Yttria-stabilized zirconia (YSZ) has been

chosen for the proposed experiments because of its availability and its low electronic conductivity.<sup>(15)</sup>

The ionic conductivity of the YSZ solid electrolyte can be used in an electrochemical cell to measure the thermodynamic activity of oxygen in liquid  $\text{Pb}_{1-x}\text{Sn}_x\text{Te}$ . The cell is represented by



where M and  $\text{M}_m\text{O}$  represent a metal and its oxide for which the Gibb's free energy of formation,  $\Delta G_f^\circ(\text{M}_m\text{O})$ , is accurately known. The partial pressure of oxygen on the reference side of the electrolyte,  $P(\text{O}_2)(\text{reference})$ , is known from the equilibrium relationship

$$\Delta G_f^\circ(\text{M}_m\text{O}) = RT \ln P(\text{O}_2, \text{reference})^{1/2}, \quad (7)$$

where R is the gas constant, T is the absolute temperature, and the partial pressure is measured in atmospheres. In eq. 6,  $[\text{O}]$  represents atomic oxygen dissolved in the liquid  $\text{Pb}_{1-x}\text{Sn}_x\text{Te}$  sample; its thermodynamic activity is  $a_0(\text{sample})$ . The Nernst equation relates the thermodynamic properties of the cell to the potential, E, that can be measured across the cell:

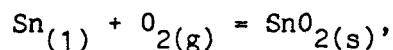
$$E = \frac{RT}{2F} \ln \frac{(P(\text{O}_2, \text{reference}))^{1/2}}{a_0(\text{sample})^{1/2}}, \quad (8)$$

F representing the Faraday constant.<sup>(16)</sup> Equations 7 and 8 can be combined to obtain

$$E = (1/2F)[\Delta G_f^\circ(M_mO) - RT \ln a_O(\text{sample})]. \quad (9)$$

Since  $a_O(\text{sample})$  is a function of the oxygen concentration in the liquid, the measured cell potential reveals the oxygen concentration. The meaning of eq. 9 can also be reversed: an arbitrary potential applied across the electrochemical cell will pump oxygen ions through the electrolyte until an equilibrium is reached, with the oxygen activity and concentration in the sample corresponding to the applied potential. If the cell and the applied potential are in a series circuit, the number of ions transferred through the electrolyte can be found by measuring the number of electrons that travel through the circuit; that is, by measuring the current in the circuit.<sup>(17,18)</sup> This is the electrochemical titration technique. It is proposed that oxygen be used as a tracer element in a  $Pb_{1-x}Sn_xTe$  sample; that the tracer be added to the sample by titration with one cell and detected by a second cell. The response at the detection cell to an input at the titration cell as a function of time will then reveal the nature of the convective flow in the sample between the two cells.

The solubility of oxygen in  $Pb_{1-x}Sn_xTe$  is finite and if it is exceeded the elements in the sample begin to form oxides. The first oxide to form is the one with the lowest  $\Delta G_f^\circ$ , tin(IV) oxide ( $SnO_2$ ). Once the oxide is formed the activity and the partial pressure of oxygen in the sample electrode are fixed by the equilibrium of the reaction



$$\Delta G_f^\circ(SnO_2) = RT \ln [a_{Sn} P(O_2, \text{sample})]. \quad (10)$$

Equation 4 can also be written as

$$E = \frac{RT}{2F} \ln \frac{P(O_2, \text{reference})^{1/2}}{P(O_2, \text{sample})^{1/2}}, \quad (11)$$

and eq. 10 and 11 combined form

$$E = (1/2F)[\Delta G_f^\circ(M_mO) - 1/2 \Delta G_f^\circ(SnO_2) + 1/2RT \ln a_{Sn}]. \quad (12)$$

Thus the cell potential in this case can be related to the activity and hence the concentration of tin in the  $Pb_{1-x}Sn_xTe$  sample. Composition profiles are measured in solid samples after crystal growth; the electrochemical cell can provide data on the liquid composition during growth.

An important part of the preparatory work for the proposed experiments has been the selection of the materials that will be used in the electrochemical cells. An early choice was the chemical system to be used as the reference electrode. Gas electrodes (air,  $O_2$ , or a gas mixture) are commonly used in solid electrolyte electrochemical cells,<sup>(13,17)</sup> but were in this case rejected because of the difficulty involved in keeping the molten liquid sample electrode separate from the gas reference electrode. A solid reference electrode can be more easily assembled and sealed, so the initial choice for the reference electrode was the often-used nickel-nickel oxide (Ni-NiO) system.<sup>(19-22)</sup> This system is well-defined thermodynamically and has a partial pressure of oxygen relatively near that expected in the sample electrode, which prevents excessive oxidation of the sample.<sup>(23)</sup> However, the resistance of the Ni-NiO system to electric current and oxygen transfer, which leads to error in the cell potential measurement, is more than is desired and the copper-copper (I) oxide system ( $Cu-Cu_2O$ ) is being considered as an alterna-

tive.<sup>(24-25)</sup> The next choice was the material for the electrical contacts from each electrode to the measuring instruments. It is essential that the contact materials and the electrodes be sufficiently inert towards each other for long periods of time at high temperatures. Experiments have shown that tungsten wire can be used in both liquid tin and in Ni-NiO, while the best contact material for  $\text{Pb}_{1-x}\text{Sn}_x\text{Te}$  appears to be graphite. Experiments with Cu-Cu<sub>2</sub>O have not yet been conducted. The accuracy and effective lifetime of a cell are greatly enhanced if it is not allowed to oxidize. To this end the cell is sealed away from air and is ventilated with argon gas which has passed through a three-step purification line: first, hydrogen is catalytically reacted with oxygen to form water, then all water is removed by a dessicant, and finally the remaining oxygen is reacted with titanium at 850°C. The resulting argon has an oxygen partial pressure of about  $10^{-33}$  atm. while the expected oxygen partial pressure of the electrochemical cell is about  $10^{-11}$  atm.

The proposed experiments require two types of electrochemical cells. First a single cell, shown in Figure 4, will be used to measure the electrical potential (and therefore the thermodynamic activity of oxygen in the liquid) as a function of oxygen concentration. The measurement will be done by electrochemically removing as much oxygen as possible from the liquid sample, then titrating oxygen back in while observing the changing cell potential. Once the liquid is saturated the solubility of oxygen in the liquid is known. The results from the single cell experiments form the data base required for the convection experiments using a double cell, shown in Figure 5. The idea for the double cell arrangement is from Otsuka and Kozuka.<sup>(20)</sup> In the double cell the sample is in a vertical cylinder, with an electrolyte at the bottom face that functions as an oxygen pump cell and an electrolyte at the top face that

functions as an oxygen detector cell. Transport of oxygen through the liquid sample between the electrolytes is measured by observing the response at the detector cell to a step or pulse input of oxygen at the pump electrode. The measurement will be made under two conditions: an isothermal condition where convection is minimal and oxygen transport is chiefly by diffusion, and a temperature gradient condition, where oxygen transport is by diffusion and convection. The first condition will permit the calculation of the diffusion coefficient of oxygen in the liquid<sup>(20)</sup> and the second condition will, by comparison to the first condition, reveal the bulk effect of convection in the liquid.

The proposed experiments will give a thorough understanding of the activity, solubility, and diffusivity of oxygen in  $\text{Pb}_{1-x}\text{Sn}_x\text{Te}$  and can form the basis for further research. For example, in Bridgman crystal growth the shape of the solid-liquid interface has a strong effect on the convective flow patterns in the liquid,<sup>(7)</sup> but it is difficult to discover experimentally the shape of the interface. By using the electrochemical cell as an oxygen pump during crystal growth, the liquid can be doped with oxygen just long enough for an oxygen-rich layer of solid to be deposited at the interface. After solidification is complete the oxygen in the solid can be detected and the shape of the oxygen-rich layer will show the shape of the solid-liquid interface. Another application of electrochemical cells is to use small (less than 7mm diameter) zirconia tubes as point detectors of oxygen. These detectors are small enough to be located at various sites in the liquid to more thoroughly map the convective flow patterns in the sample. There is also potential for industrial applications of electrochemical cells, where they may be used for precise control of the concentration of oxygen as a dopant in semiconductor materials.



It would also be very interesting to test the LTT system to see if the temperature and concentration are locked "in phase" as the governing equations suggest. For this, it will be necessary to measure concentration as well as temperature. Until now, this has been difficult in semiconductor melts. It is hoped that the new electrochemical cell technique can be used to measure the concentration of the melt while temperature readings are being made with thermocouples.

Low gravity crystal growth also introduces new possibilities and some new problems. For example, containerless crystal growth is a promising method for space processing. Buoyancy-driven flow will be eliminated due to the low values of  $g(-10^{-3} g_{\text{earth}})$  and crystal defects due to wall-melt interactions will be eliminated. But the resulting gas-liquid surface, in the presence of a temperature gradient, will be subject to Marangoni convection. On the other hand, in conventional growth with side walls, Marangoni convection will not be a problem, but convection may result from the density change upon freezing. If  $\epsilon$  is large, there will be a net flow of fluid towards the interface. This flow will not be uniform, due to the no-slip condition at the wall. So even though buoyancy is nearly eliminated there are still driving forces for convection in space. Perhaps the melt can be encapsulated in another liquid phase. The lower shear at the phase boundary will allow nearly even fluid flow to the interface and there will be no free surface available for Marangoni convection. This is just one example of the type of problem that may be investigated in the future.

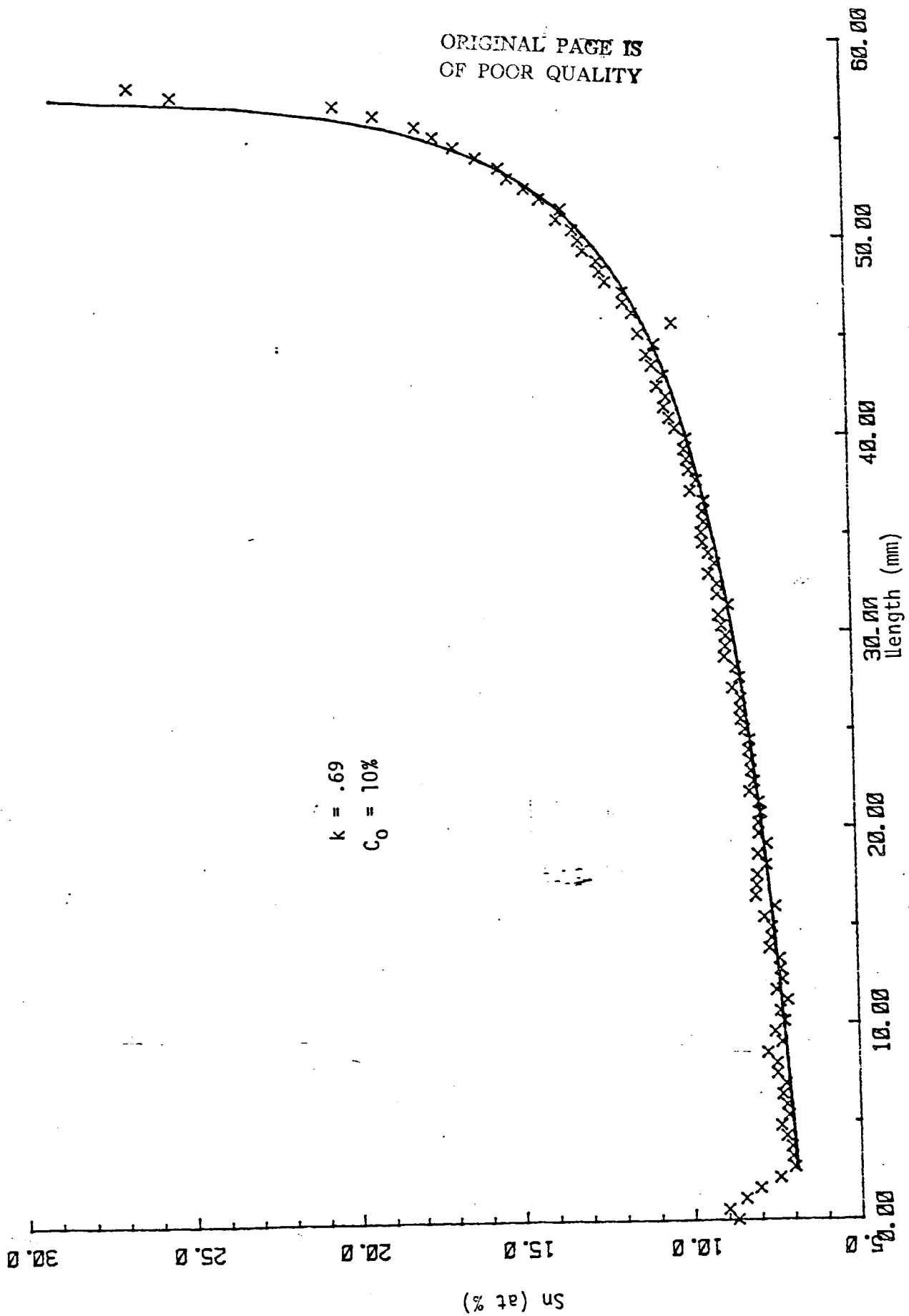


Figure 1. Compositional profile of PbSnTe sample. The solid line is a plot of the Scheil equation.

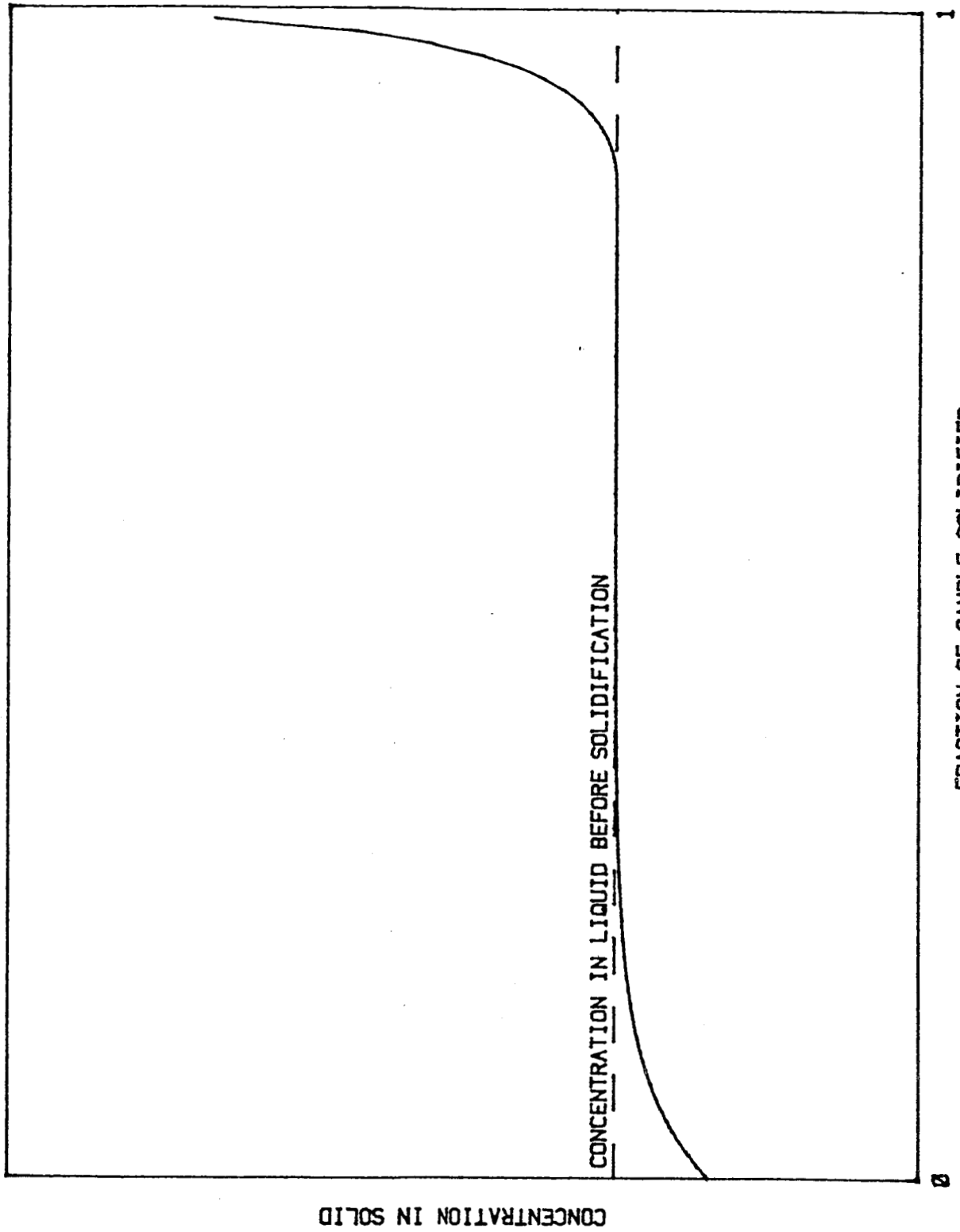


Figure 2. Theoretical concentration curve for diffusion-only solidification (from Reference 4).

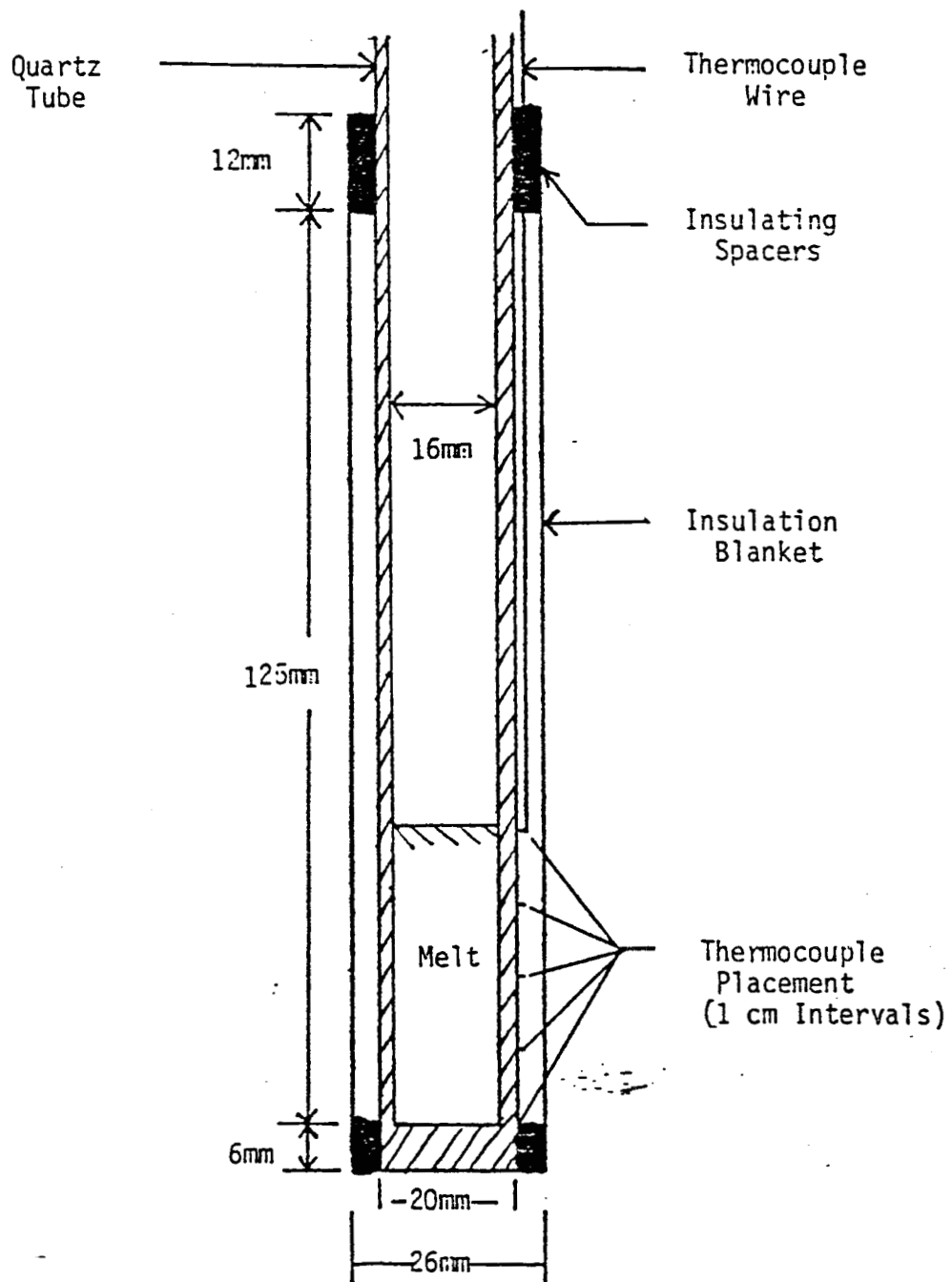


Figure 3. Diagram of Bridgman Tube.

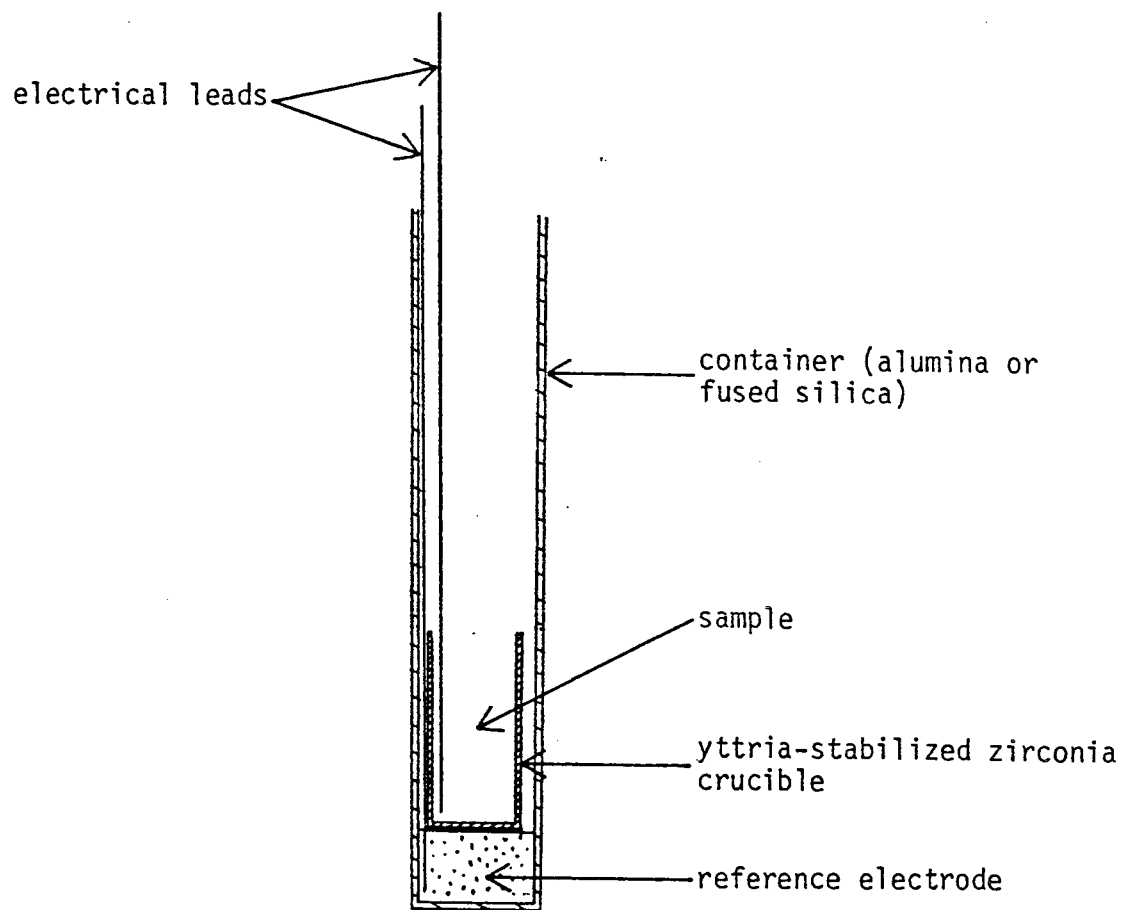


Figure 4. Single electrochemical cell assembly.

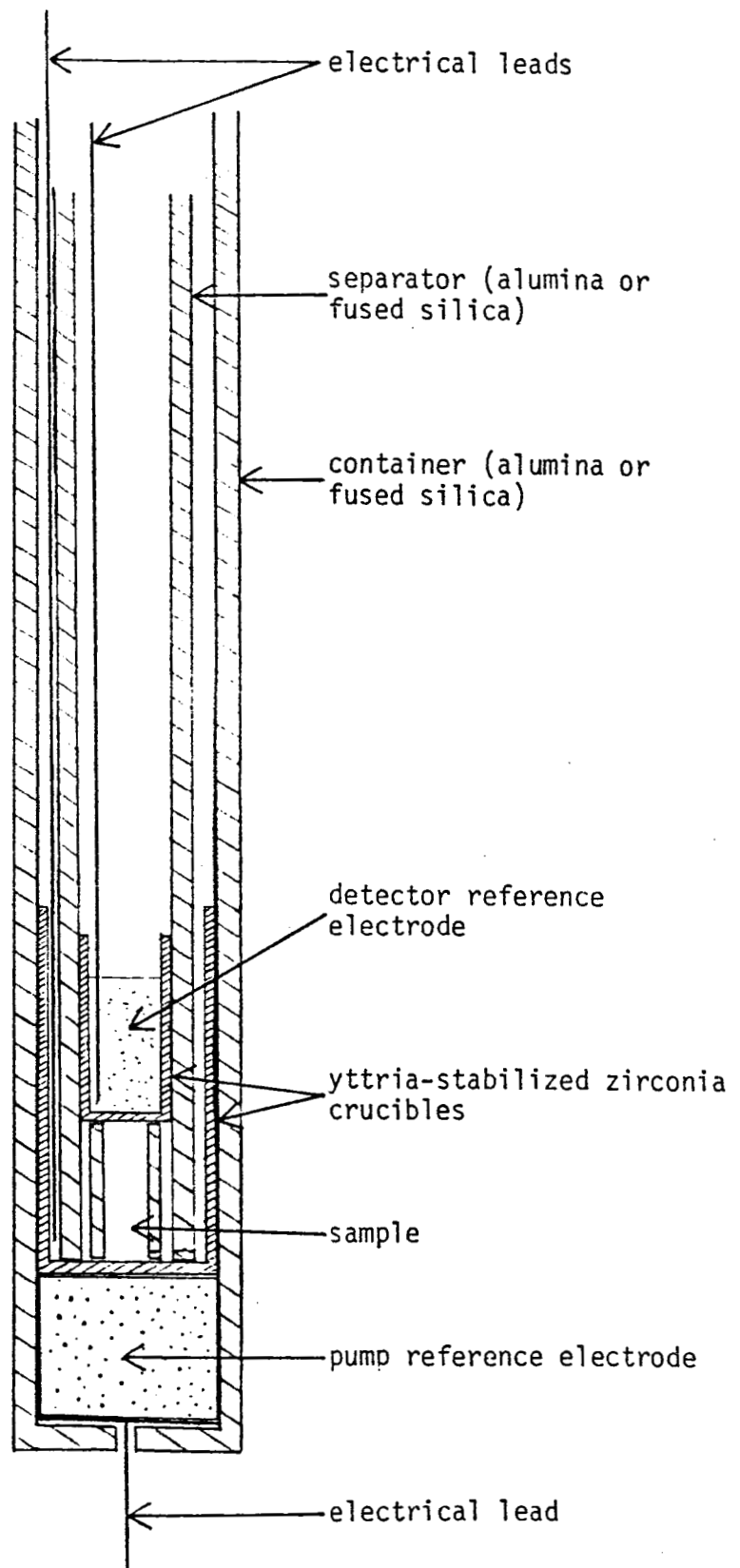


Figure 5. Double electrochemical cell assembly.

# REFERENCES

1. Kressel, H., and Butler, J.K., Semiconductor Lasers and Heterojunction LED's, New York: Academic Press (1977), p. 439.
2. Harris, J.S., Longo, J.T., Gertner, E.R., and Clarke, J.E., J. Crystal Growth, 28 (1975), p. 334-342.
3. Pamplin, B.R., "Introduction to Crystal Growth Methods," Crystal Growth, 2nd ed., B.R. Pamplin, ed., New York: Pergamon Press (1980), p. 8.
4. Tiller, W.A., Jackson, K.A., Rutter, J.W., and Chalmers, B., Acta Metallurgica, 1 (1953), pp. 428-437.
5. Crouch, R.K., Fripp, A.L., Debnam, W.J., Clark, I.O., Barber, P.G., and Carlson, F.M., Acta Astronautica, 12 (1985), pp. 923-929.
6. Vrentas, J.S., Narayanan, R., and Agrawal, S.S., Int. J. Heat Mass Transfer, 24 (1981), pp. 1513-1529.
7. Carlson, F.M., Fripp, A.L., and Crouch, R.K., J. Crystal Growth, 68 (1984), pp. 747-756.
8. Carlson, F.M., Technical Report for NASA Grant No. NAG-1-397, July 28, 1986.
9. Schlüter, A., Lortz, D., and Busse, F., J. Fluid Mech., 23 (1965), p. 129.
10. Hoard, C.Q., Robertson, C.R., and Acrivos, A., Int. J. Heat Mass Transfer, 13 (1970), p. 849.
11. Fu, T.W., and Wilcox, W.R., J. Crystal Growth, 48 (1980), p. 416.
12. Rouzaud, A., Camel, D., and Favier, J.J., J. Crystal Growth, 73 (1985), p. 149.
13. Rapp, R.A., and Shores, D.A., "Electrochemical Measurements: Solid Electrolyte Galvanic Cells," Physicochemical Measurements in Metals Research, Part 2, R.A. Rapp, ed., New York: Interscience Publishers (1970), pp. 123-192.
14. McGeehin, P., and Hooper, A., J. Mater. Sci., 12 (1977), pp. 1-27.
15. Dixon, J.M., LaGrange, L.D., Merten, U., Miller, C.F., and Porter, J.T. II, J. Electrochem. Soc., 110 (1963), pp. 276-280.
16. Kiukkola, K., and Wagner, C., J. Electrochem. Soc., 104 (1957), pp. 379-387.
17. Ramanarayanan, T.A., and Rapp, R.A., Metal. Trans., 3 (1972), pp. 3239-3246.

18. Otsuka, S., and Kozuka, Z., Trans. Japan Inst. Metals, 25 (1984), pp. 639-648.
19. Charette, G.G., and Flengas, S.N., J. Electrochem. Soc., 115 (1968), pp. 796-804.
20. Otsuka, S., and Kozuka, Z., Metal. Trans., 6B (1975), pp. 389-394.
21. Alcock, C.B., and Belford, T.N., Trans. Faraday Soc., 60 (1964), pp. 822-835.
22. Belford, T.N., and Alcock, C.B., Trans. Faraday Soc., 61 (1965), pp. 443-453.
23. Ramanarayanan, T.A., and Worrell, W.L., Unpublished paper, (1973).
24. Worrell, W.L., National Bureau of Standards Special Publication 455, Electrocatalysis on Non-Metallic Surfaces, (1976), pp. 351-358.
25. Ramanarayanan, T.A., and Worrell, W.L., Metal. Trans., 5 (1974), pp. 1773-1777.